

# A Frequency-EBIC Technique for High Spatial Resolution of the Effective Minority Charge Carrier Lifetime in SiC PN-Junctions

Christian Stefan Gruber<sup>1,2,a\*</sup>, Gregor Pobegen<sup>1,b</sup> and Jürgen Smoliner<sup>2,c</sup>

<sup>1</sup>Kompetenzzentrum für Automobil- und Industrieelektronik GmbH, Europastraße 8, 9524 Villach, Austria

<sup>2</sup>Technische Universität Wien, Institute of Solid State Electronics, Gußhausstraße 25-25a, 1040 Wien, Austria

<sup>a\*</sup>christianstefan.gruber@k-ai.at, <sup>b</sup>gregor.pobegen@k-ai.at, <sup>c</sup>juergen.smoliner@tuwien.ac.at

**Keywords:** recombination lifetime, minority charge carrier lifetime, effective lifetime, scanning electron microscope, electron beam induced current, time-resolved EBIC.

**Abstract.** We present a new method to potentially map the effective minority charge carrier lifetime by means of a chopped electron beam induced current in a scanning electron microscope using a digital lock-in amplifier. While previous authors have been mainly interested in measuring the diffusion length and some even the minority charge carrier lifetime using line-scans, we show that this method could be extended to measure the lifetime locally in the cross section of a given device. In our case, we use a simple SiC pn-junction. The decrease of current with increasing chopping frequency of the electron beam makes a direct measurement of the effective lifetime possible. Inspired by optical beam induced current (OBIC), this novel approach has great potential to measure the minority charge carrier lifetime locally and is going to help device and process engineers to develop the next generation of SiC power devices.

## Introduction

The effective minority charge carrier lifetime is a crucial parameter that influences a plethora of device characteristics, most notably reverse recovery and in consequence, the switching speed of a power device. For future optimization in both device and process engineering, this raises the question and the need to accurately measure the effective lifetime not only of an entire device, which may be seen as an integrated measurement of all local lifetimes combined, but locally. Existing optical methods include time-resolved photoluminescence [1], time-resolved photoconductance [2] measurements but none of these methods reach sub-micron resolution. A scanning electron microscope (SEM) outperforms optical excitation setups by orders of magnitude in terms of spot size. Thus, a scanning electron microscope can be used in order to obtain the effective minority charge carrier lifetime with great spatial resolution.

The phenomenological process of recombination may be split up into the following physical processes: Shockley-Read-Hall, radiative, Auger-Meissner and surface recombination [3].

These recombination effects can also be written in terms of their corresponding lifetime: Shockley-Read-Hall (SRH)  $\tau_{\text{SRH}}$ , radiative  $\tau_{\text{rad}}$  and Auger-Meissner  $\tau_{\text{Aug}}$  lifetime. Surface recombination  $\tau_{\text{sur}}$  also needs to be considered:

$$\frac{1}{\tau_{\text{eff}}} = \frac{1}{\tau_{\text{SRH}}} + \frac{1}{\tau_{\text{rad}}} + \frac{1}{\tau_{\text{Aug}}} + \frac{1}{\tau_{\text{sur}}} \quad (1)$$

In terms of their physics, SRH describes the recombination of electron-hole pairs through deep level impurities or traps. The energy that is set free during the process is mediated by phonons. Radiative recombination describes a direct band-to-band transition, whose energy is set free by a photon. For intrinsic SiC (without doping), radiative recombination however is unlikely due to its indirect band gap. Radiation may however be emitted through optical transitions of point defects in the crystal. Auger-Meissner recombination is a three-particle process. When an eh-pair recombines, the transition

energy is given off to an outer shell electron, resulting in the ionization of the atom. Surface recombination is a phenomenon that occurs at semiconductor interfaces to other media (such as air or other dielectrics). The crystal lattice is abruptly disturbed. Dangling bonds at this interface become traps for eh-pairs [3] and lead to rapid recombination and short lifetimes near the surface.

Accounting for all recombination processes separately needs labor-intensive measurements, while usually the effective carrier lifetime  $\tau_{\text{eff}}$  is sufficient in most cases to optimize the device according to the need of the device engineer and subsequently the application.

## Theory

In our effective lifetime measurements, we use the well-known technique called electron beam induced current (EBIC). An incident electron beam on a semiconductor sample creates electron hole pairs. If an electric field is present (like the electric field of a depletion region), the eh-pairs are separated efficiently and can be measured in an external electrical circuit (see Fig. 2). EBIC is used in many applied fields such as failure analysis or defect characterization. Theoretically, it can best be described by the diffusion equation [4] for minority carriers in a n-doped material (same considerations apply for a p-doped material):

$$D_p \frac{\partial(p_n - p_{n0})}{\partial x^2} - \frac{p_n - p_{n0}}{\tau_p} = \frac{\partial p_n - p_{n0}}{\partial t} \quad (2)$$

Here,  $D_p$  is the diffusion coefficient,  $p_n - p_{n0}$  the excess carrier concentration and  $\tau_p$  the effective carrier lifetime. Steady-state EBIC is by far the most common technique. Therefore, in steady-state, the right-hand side of Eq. 2 is 0 and we get the well-known solution  $I_{\text{EBIC}} \propto \exp\left(\frac{-x}{L_p}\right)$ , where  $L_p = \sqrt{D_p \tau_p}$  is the diffusion length. Since in the following analysis, we are concerned with a frequency-dependent approach, the excess carrier concentration oscillates with a given frequency, thus making a time-dependent approach necessary [4]:

$$u(x) = (p_n - p_{n0})e^{i\omega t} \quad (3)$$

$u(x)$  is the general solution to the diffusion Eq. 2 may now be rewritten:

$$\frac{d^2 u}{dx^2} - \frac{1}{L_p} (1 + i\omega \tau_p) u(x) = 0 \quad (4)$$

This differential equation may be solved, yielding the following general solution (using  $\omega = 2\pi f$ )

$$u(x) = A \exp\left(\frac{x}{L_p} (\beta + i\gamma)\right) + B \exp\left(-\frac{x}{L_p} (\beta + i\gamma)\right) \quad (5)$$

with

$$\beta, \gamma = \frac{1}{\sqrt{2}} \sqrt{\pm 1 + \sqrt{1 + (2\pi f \tau_p)^2}}. \quad (6)$$

The coefficient A is zero, because far away from the junction, EBIC should be null. The phase  $\gamma$  has a minus sign, such that the phase becomes zero in steady-state ( $f = 0$ ). This short mathematical derivation already gives some interesting theoretical insights into the semiconductor material and the EBIC signal and its corresponding phase. This relationship between EBIC, phase and distance are plotted in Fig. 1. With an increase of the beam blanking (chopping) frequency of the electron beam, the EBIC signal is expected to decrease, while the phase becomes more negative. From this decrease in EBIC, the effective carrier lifetime  $\tau_p$  may be determined. The same information can be obtained from the phase  $\gamma$ .

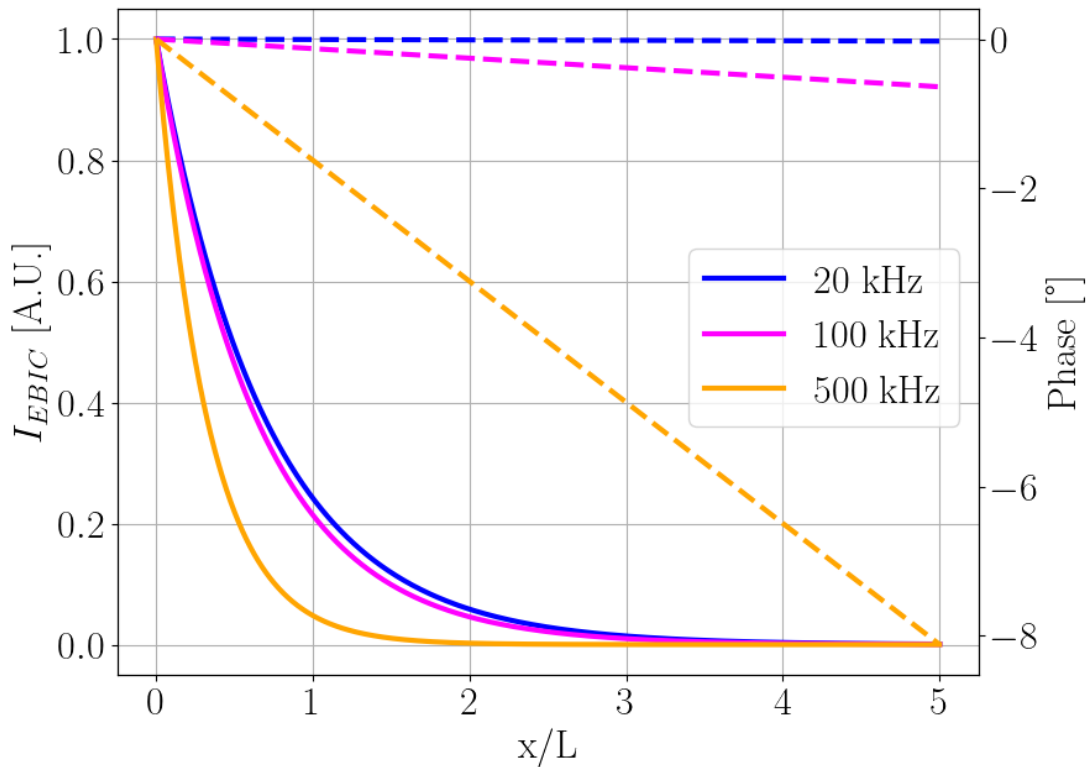


**Fig. 1.** Theoretical EBIC signal prediction of a carrier lifetime of  $1 \mu\text{s}$  for increasing distance  $x$  from the depletion region scaled by the diffusion length  $L$ . Solid lines denote the current, dashed lines are the phase prediction for different frequencies. The higher the chopping frequency, the smaller the EBIC signal response with increasing distance (left scale), following Eq. 5. Simultaneously, the phase (right hand scale, dotted straight lines) becomes more negative with increasing frequency.

Plotting the EBIC response in the frequency domain is another method to determine the effective lifetime, as is depicted in Fig. 1. Fig. 1 neglects the surface contribution to the EBIC signal. In a real experiment, the EBIC signal is affected by surface recombination, altering the minority charge carrier lifetime. This surface effect can however be accounted for quantitatively, using the technique of Pang et. al. [5]. This method may be altered to use different acceleration voltages for the electron beam (probing depths) as interpolation points to determine the diffusion coefficient and the surface recombination velocity locally.

Another well-known method is time-resolved cathodoluminescence (same principle as time-resolved photoluminescence), which is however limited to measure the radiative carrier lifetime only.

## Method

While the previous analysis has been performed by numerous authors [6, 7, 8] using time-resolved EBIC in the 1980s and very recently by Vasco et. al. [9], local measurement and comparison near the depletion region of minority charge carrier lifetime using the frequency-EBIC method on device level has not been done to our knowledge. After background subtraction at a particular position  $x$ , we compare the normalized data of a low and high frequency domain EBIC to deduce the local effective lifetime anywhere in the device:

$$r = \frac{\log(I_{500\text{kHz}})}{\log(I_{20\text{kHz}})} = \frac{\frac{-x}{L_p\sqrt{2}} \sqrt{\pm 1 + \sqrt{1 + (2\pi f_{500\text{kHz}}\tau_p)^2}}}{\frac{-x}{L_p\sqrt{2}} \sqrt{\pm 1 + \sqrt{1 + (2\pi f_{20\text{kHz}}\tau_p)^2}}} \quad (7)$$

We expect  $\tau_p$  to be in a range of roughly  $10^{-7} - 10^{-6}$  s far away from the depletion region, such that the product  $f_{20\text{kHz}}\tau_p$  is negligible (the error being around 0.2 % for a lifetime of 1  $\mu\text{s}$ ), such that we can write:

$$r = \frac{1}{\sqrt{2}} \sqrt{1 + \sqrt{1 + (2\pi f_{500\text{kHz}}\tau_p)^2}} \quad (8)$$

One could potentially measure the steady state EBIC with a regular DC-EBIC amplifier instead. However, using two different measurement instruments can yield erroneous results in the magnitude (such as offsets and differences in the amplification factor). From an application standpoint, low frequencies also require long averaging times, since lower frequencies have longer periods. To average over the same number of periods thus requires more time. In consequence, the beam needs to dwell at point  $(x_i, y_i)$  until the lock-in amplifier has successfully done its averaging and returned the signal into the SEM before the beam may move to position  $(x_{i+1}, y_i)$ . Otherwise, the lock-in signal becomes a mix of EBIC at  $(x_i, y_i)$  and  $(x_{i+1}, y_i)$  which is generally undesired.

Eq. 8 can easily be rewritten in terms of  $\tau_p$ :

$$\tau_p = \frac{\sqrt{(2r^2 - 1)^2 - 1}}{2\pi f_{500\text{kHz}}} \quad (9)$$

This derivation has one flaw: The diffusion length  $L_p$  as well as the lifetime  $\tau_p$  are considered constants with respect to  $x$  in the analytical solution made by McKelvey. Here, first the diffusion Eq. 2 is solved with constant  $L_p$  and  $\tau_p$ , but we then change our view and assume it to be dependent on  $x$ .

## Experimental Setup

In our experiment, a Thermo Fisher Apreo 2 with a Zurich Instruments HFLI Lock-In Amplifier was used. The blanking capability of the Thermo Fischer Apreo 2 SEM is limited by a 20 ns rise/fall time, which gives a highest usable frequency of 100 MHz. The usable frequency range is much lower due to parasitic capacitances in the cables and measurement electronics. The setup is depicted in Fig. 2: A reference signal of the lock-in amplifier was fed into the beam blanking electronics of the SEM. The beam is thus blanked at a desired frequency  $f$ . The chopped beam hits the sample and creates eh pairs which diffuse towards the nanoprobe needle or chuck on the back of the sample. This EBIC shown in (c) is then measured in the lock-in amplifier. Meanwhile, it is always possible to obtain a secondary electron image such as from the separated Everhardt-Thornley detector (ETD) as depicted in (b).

As shown in Fig. 2 (d), one could potentially sweep all available frequencies to obtain the entire low-pass filter behavior of a certain position. Since this procedure is quite laborious, it is sufficient to pick two suitable EBIC images taken at two different carefully chosen frequencies (ideally one low frequency and one large one without neglecting the limitations of the SEM, cables and lock-in amplifier).

## Results

Our sample is a high bandgap SiC diode. The most important physical properties are summarized in Table 1. The depletion layer thickness and electric field were calculated from the available doping concentrations and voltage drop.

**Table 1.** Physical properties of the investigated SiC pn-junction.

p-region doping concentration (cm <sup>-3</sup> )	10 <sup>18</sup> (Al)
p-region thickness (nm)	400
epitaxial layer doping concentration (cm <sup>-3</sup> )	10 <sup>16</sup> (N)
epitaxial layer thickness (nm)	5000
Voltage drop (V)	2.93

Within the depletion region, speaking of a minority charge carrier lifetime originating from a diffusion current is misleading. In the depletion region, this process is not dominated by diffusion but by a drift current. When an eh-pair is generated in the depletion region, the electric field and not a diffusion current accelerates the electrons and holes towards their respective oppositely charged junction boundaries (much like in a plate capacitor). In this analysis, we talk of this time as the transit time  $t$  from the generation of a charged carrier to the border of the depletion region and not as the minority carrier lifetime.

Using the mobilities  $\mu_{p,n}$  of electrons and holes in SiC (900 and 100  $\frac{\text{cm}^2}{\text{Vs}}$  respectively), the transit time through the depletion region can be computed easily. The velocity  $v = \mu E$  [10] can also be rewritten in terms of  $v = w/t$ ,  $w$  being the depletion width. We computed a transit time in the range of picoseconds. Even though these calculations are at best approximate, one can deduce that these transit times are much smaller than the effective minority carrier lifetimes measured in the following analysis. It can thus be assumed that when an eh-pair is generated in the depletion region, it is first swept across the depletion region before it can be measured as current in the external circuit, as majority carriers. The effective minority charge carrier lifetime of generated minority charge carriers on their path towards the depletion region is what we can measure in this analysis, not when carriers are generated within the depletion region. A possible subject for further investigation is bias dependence of EBIC: One could apply a small forward bias (not greater than the built-in voltage) or reverse bias to the junction, such that the depletion region shrinks or expands. That way, the minority charge carrier lifetime closer or further away from the abrupt pn-junction could be analyzed, bearing in mind that the voltage drop only occurs at the depletion region boundary. These experiments have however not been performed yet and will be investigated in the future.

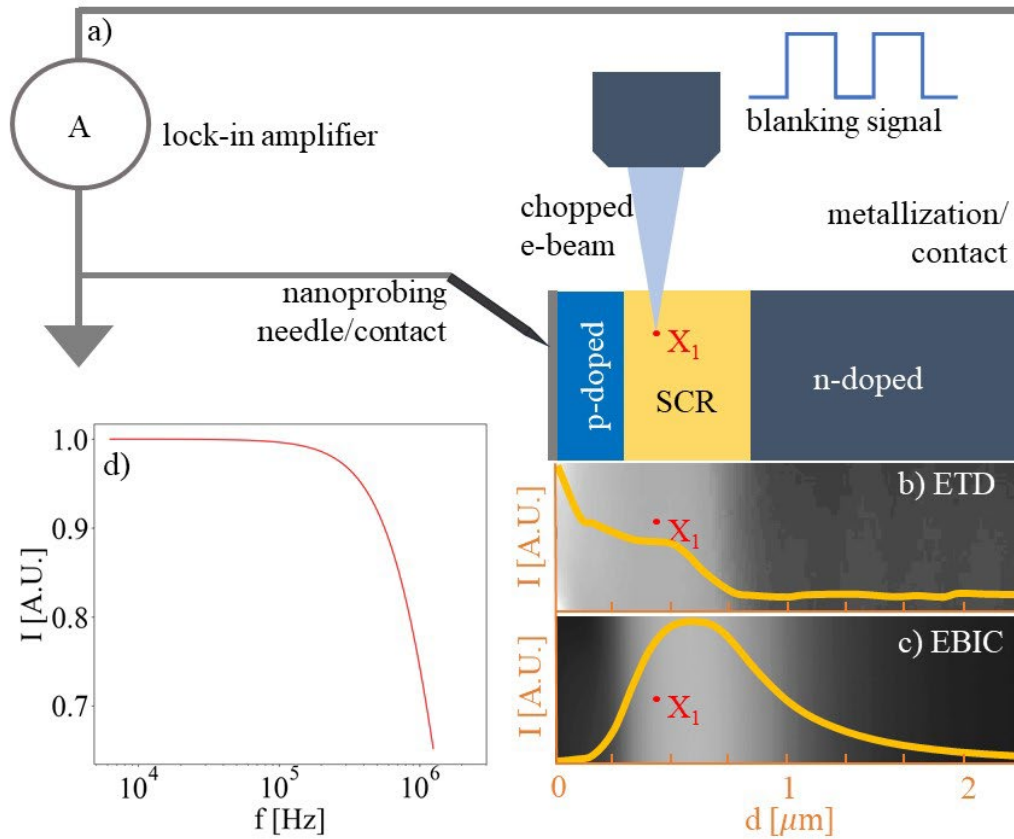


**Fig. 2.** Schematic of the experimental setup: a) The beam is blanked by the reference signal of the lock-in amplifier. If the eh-pairs are generated close enough to the depletion region, they can diffuse to the respective contact pads/back metallization respectively, and be recorded by the lock-in amplifier. Simultaneous measurements (b) of secondary electrons (SE) in the Everhardt-Thornley Detector (ETD) and (c) EBIC is common to yield secondary electron and EBIC images from the scanning of the electron beam over a region of interest. d) Frequency dependence of the EBIC current at position  $X_1$ . As stated, we refrain from performing an entire sweep of frequencies, but rather compare a low and high frequency EBIC image, which is sufficient to create effective lifetime maps.

By stacking two EBIC images on top of each other, the ratio  $r$  and subsequently  $\tau_p$  can be obtained from Eq. 9, as depicted in Fig. 3. While strictly only two frequency-dependent EBIC (fEBIC) images are necessary to obtain the minority charge carrier lifetime, some line scans were obtained to show the characteristic decrease of EBIC with increasing frequencies.

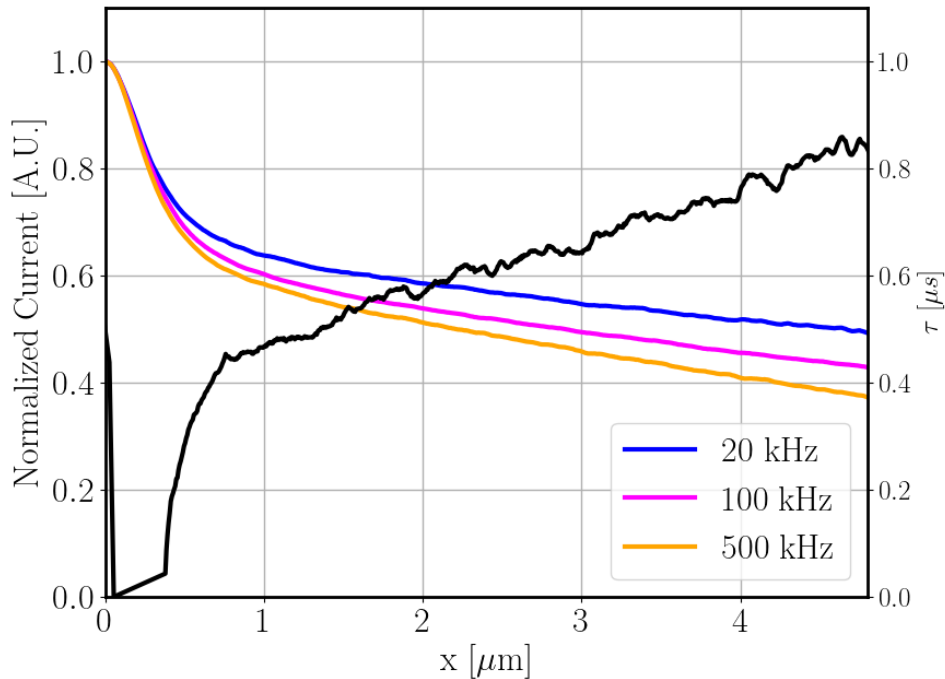


**Fig. 3.** Frequency-dependent normalized EBIC current (at 10kHz, 20 kHz, 100 kHz and 500 kHz) and the respective minority charge carrier lifetime (in red) of line-scans using Eq. 9. The bump in lifetime close to zero is a result of computing a value close to  $\log(1) = 0$ .

### Summary and Outlook

We have shown that the effective minority charge carrier lifetime can be computed locally in the cross section of a device which may provide valuable information of recombination characteristics. Here, we only use line-scans to measure the lifetime locally, however this technique can be extended to measure the lifetime anywhere in a device, since this technique does not require the knowledge of  $x$  or  $L$ . While this novel technique has great potential to be used in future failure analysis and device optimization techniques, there are still some unsolved challenges to overcome until this method is ready to be fully automated. Once this method runs smoothly everywhere in the cross section, we will be using different accelerating voltages to compute both the diffusion coefficient and the surface recombination velocity locally.

### Acknowledgement

This work was funded by the Austrian Research Promotion Agency (FFG, Project No. 914019).

### References

- [1] Li, Z., Liu, A., Basnet, R., Black, L. E., Macdonald, D., & Nguyen, H. T. (2025). Applications of time-resolved photoluminescence for characterizing silicon photovoltaic materials. *Semiconductor Science and Technology*, 40(4), 045015.
- [2] Sanders, A., & Kunst, M. (1991). Characterization of silicon wafers by transient microwave photoconductivity measurements. *Solid-state electronics*, 34(9), 1007-1015.
- [3] D. K. Schroder, *Semiconductor Material and Device Characterization*, third ed., John Wiley & Sons, Hoboken, 2006.

- [4] J. P. McKelvey, Solid state and semiconductor physics, Robert E. Krieger Publishing Company, Malabar, 1966.
- [5] S. Pang, A. Rohatgi, A new methodology for separating Shockley-Read-Hall lifetime and Auger recombination coefficients from the photoconductivity decay technique, Journal of applied physics, 74 (1993) 5554-5560.
- [6] T. Fuyuki, H. Matsunami, Determination of lifetime and diffusion constant of minority carriers by a phase-shift technique using an electron-beam-induced current, Journal of Applied Physics, 52 (1981) 3428-3432.
- [7] J. Pietzsch, Measurement of minority carrier lifetime in GaAs and GaAs(1-x)P(x) with an intensity-modulated electron beam, Solid-State Electronics, 25 (1982) 295-304.
- [8] N. Honma, C. Munakata, H. Itoh, T. Warabisako, Nondestructive Measurement of Minority Carrier Lifetimes in Si Wafers Using Frequency Dependence of ac Photovoltages, Japanese Journal of Applied Physics, 25 (1986).
- [9] S. Bustillos-Vasco, N. Baier, C. Lobre, C. Cervera, N. Péré-Laperne, A. Evirgen, O. Gravrand, Use of Electron Beam-Induced Current Technique to Characterize Transport Properties of Narrow-Gap-Energy Materials for IR Detection, Journal of Electronic Materials, 53 (2024) 5850-5857.
- [10] S. M. Sze, Y. Li and K. K. Ng, Physics of Semiconductor Devices, third ed., John Wiley & Sons, Hoboken, 2007.